Basic Study on Analysis and Suppression of Inverse Response Caused by Feedforward Friction Compensation of Ball-screw-driven Stage

Takumi HAYASHI, Hiroshi FUJIMOTO
The University of Tokyo
5-1-5, Kashiwanoha, Kashiwa, Chiba, 277-8561, Japan
hayashi.takumi18@ae.k.u-tokyo.ac.jp, fujimoto@k.u-tokyo.ac.jp

Yoshihiro ISAOKA, Yuki TERADA
DMG MORI CO., LTD.
362, Idono, Yamatokoriyama, Nara, 639-1183 Japan
yo-isaoka@dmgmori.co.jp, yk-terada@dmgmori.co.jp

***Abstract*—Ball-screw-driven stages are often used as feed systems of machine tools. A problem of tracking control of the stages is rolling friction, which degrades tracking accuracy around the velocity reversal point and causes a large tracking error called a quadrant glitch. Although the model-based feedforward friction compensation effectively reduces the tracking error, the compensation often results in an inverse response, which is the tracking error in the direction opposite to the quadrant glitch. This study aims to provide an analysis and a suppression approach to the inverse response. First, the inverse response is analyzed through the simulations. Next, a suppression approach of the inverse response is proposed. In the proposed approach, a step input is injected and cancel the inverse response. The proposed approach is evaluated through the simulations and experiments.**

***Index Terms*—Ball-screw-driven stage, rolling friction, quadrant glitch, inverse response.**

I. Introduction

Ball-screw-driven stages are often used as feed systems of industrial machines such as machine tools due to their high energy conversion efficiency, low wear, and long service life [1]. From the viewpoint of production quality, high-precision tracking control of the stages is desirable.

Despite the above requirement, the rolling friction leads to poor tracking performance of the stages. The rolling friction is generated by the balls in the ball-screw and linear guide, shown in Fig. 1. Fig. 2 shows the characteristics of the rolling friction. As shown in Fig. 2, this rolling friction depends on the displacement from the velocity reversal point. In the pre-rolling region, the rolling friction shows nonlinear elastic characteristics, while it becomes almost constant and behaves as Coulomb friction in the rolling region. Due to the rolling friction, a spike-like large tracking error occurs around the velocity reversal point. This tracking error is called a quadrant glitch.

For high-precision tracking control of the stage, it is necessary to compensate for the rolling friction and suppress the quadrant glitch. For compensation of the rolling friction, model-based and learning-based feedforward approaches are effective compared with feedback approaches, e.g., disturbance observer [2]. Many rolling friction models have been proposed

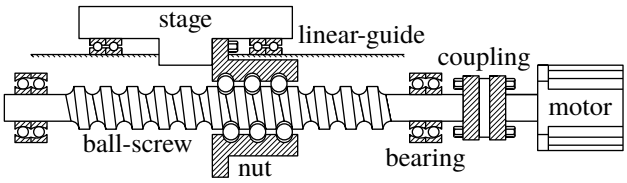

Fig. 1. Schematic of a ball-screw-driven stage. Rotational motion of the motor is converted to translational motion of the stage via the ball-screw.

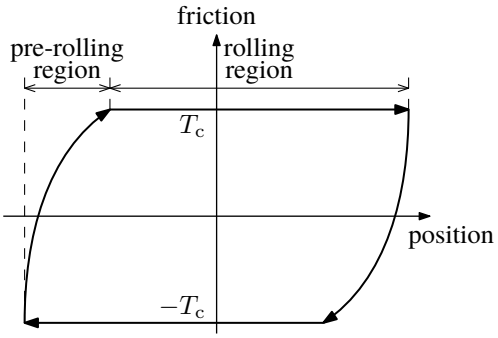

Fig. 2. Characteristics of rolling friction. Rolling friction has dependency on the displacement from velocity reversal point.

and evaluated in the literatures, e.g., LuGre model [3], generalized Maxwell-slip model [4], rheology-based model [5], data-based friction model [6], and elasto-plasticity-based model [7]. In the model-based friction compensation approaches, the rolling friction is precisely measured, and the models are obtained by curve-fitting. Then, the rolling friction is canceled with the control input calculated based on the obtained models. By contrast, the learning-based approaches, e.g., iterative learning control [8] and repetitive control [9], do not use the rolling friction models. These approaches gradually shape the compensation input and suppress the quadrant glitches by repeating the same experiments.

The above approaches efficiently suppress the quadrant glitches; however, the inverse response, which is the tracking error in the direction opposite to the quadrant glitch, is caused by the above compensation. In machining tools, the inverse

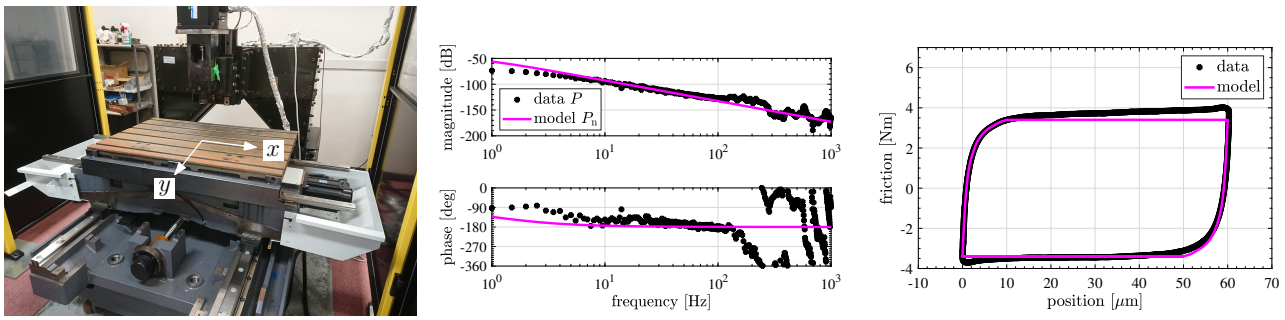

(a) Photograph. (b) Frequency response data and fitted model. (c) Measured rolling friction and fitted model.

Fig. 3. Experimental setup. In this study, only the x axis is used. The models are used in the simulations and controller design.

response causes excessive cutting and rough surface of a workpiece. This study aims to provide an analysis and a suppression approach to the inverse response. A related study is presented in [10], which deals with the inverse response caused by the friction compensation using disturbance observer. This study deals with the model-based feedforward friction compensation approach.

The remainder of this paper is organized as follows. In Section II, the experimental setup used in this study is introduced. The inverse response is confirmed in the simulations, and based on the results, an analysis of the inverse response is presented in Section III. And then, in Section IV, a suppression approach of the inverse response is proposed. This approach is verified through the simulations and experiments in Section V. Finally, the conclusions are described in Section VI.

II. Experimental Setup

Fig. 3 shows the experimental xy ball-screw-driven stage. In this study, only the x axis is used. The stage position is measured by the linear encoder with the resolution of 1 nm/pulse.

Fig. 3(b) shows the frequency response data from the motor current i [A] to the stage position x [m]. According to Fig. 3(b), the model of the stage $P_\mathrm{n}(s)$ is obtained as follows:

$$P_\mathrm{n}(s) = \frac{RK_\mathrm{T}}{J_\mathrm{n}s^2 + D_\mathrm{n}s}, \tag{1}$$

with rotation-to-translation ratio $R = 1.91\,\mathrm{mm/rad}$, torque constant $K_\mathrm{T} = 0.715\,\mathrm{Nm/A}$, nominal value of total inertia $J_\mathrm{n} = 0.015\,\mathrm{kgm^2}$, and nominal value of total viscosity coefficient $D_\mathrm{n} = 0.1\,\mathrm{Nms/rad}$. In this study, the above rigid model is employed for simplicity, while the stage is often modeled as a two-inertia system, e.g., [11]. Note that the current control of the motor is assumed to be sufficiently fast, and the delay of the current control is ignored in this study.

The characteristics of the rolling friction of the experimental setup are presented in Fig. 3(c). The rolling friction shows the nonlinear elastic characteristics in the pre-rolling region which is the range of $10\,\mu\mathrm{m}$ from the velocity reversal point, while it becomes almost constant value $T_\mathrm{c} = 3.4\,\mathrm{N\,m}$ in the rolling region.

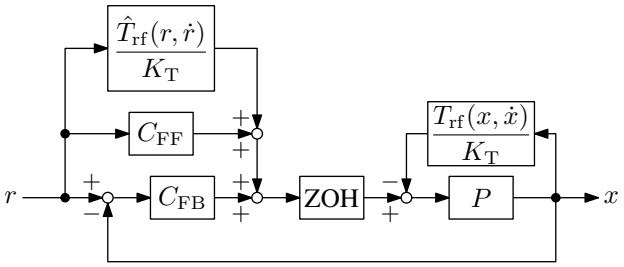

Fig. 4. Block diagram of the considered control system. Note that the rolling friction is regarded as current [A] by using the torque constant K_T.

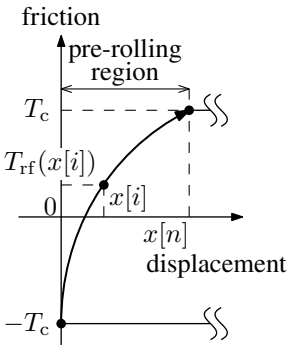

displacement	rolling friction
0	$-T_\mathrm{c}$
⋮	⋮
$x[i]$	$T_\mathrm{rf}(x[i])$
⋮	⋮
$x[n]$	T_c

Fig. 5. Data-based friction model proposed in [6]. The relation between the displacement from the velocity reversal point and the rolling friction (left figure) is represented as the table (right figure).

III. Analysis of Inverse Response in Simulation

In this section, the inverse response is observed in the simulations, and an analysis of the inverse response is presented.

A. Simulation

1) Considered Control System: The control system shown in Fig. 4 is considered. The objective of this control system is to decrease the tracking error $e = r - x$ with the position reference r and output x.

For the objective, the feedforward controller C_FF is designed as an inverse system of the model P_n, and the feedback controller C_FB is a proportional-integral-derivative (PID) controller to avoid steady-state error.

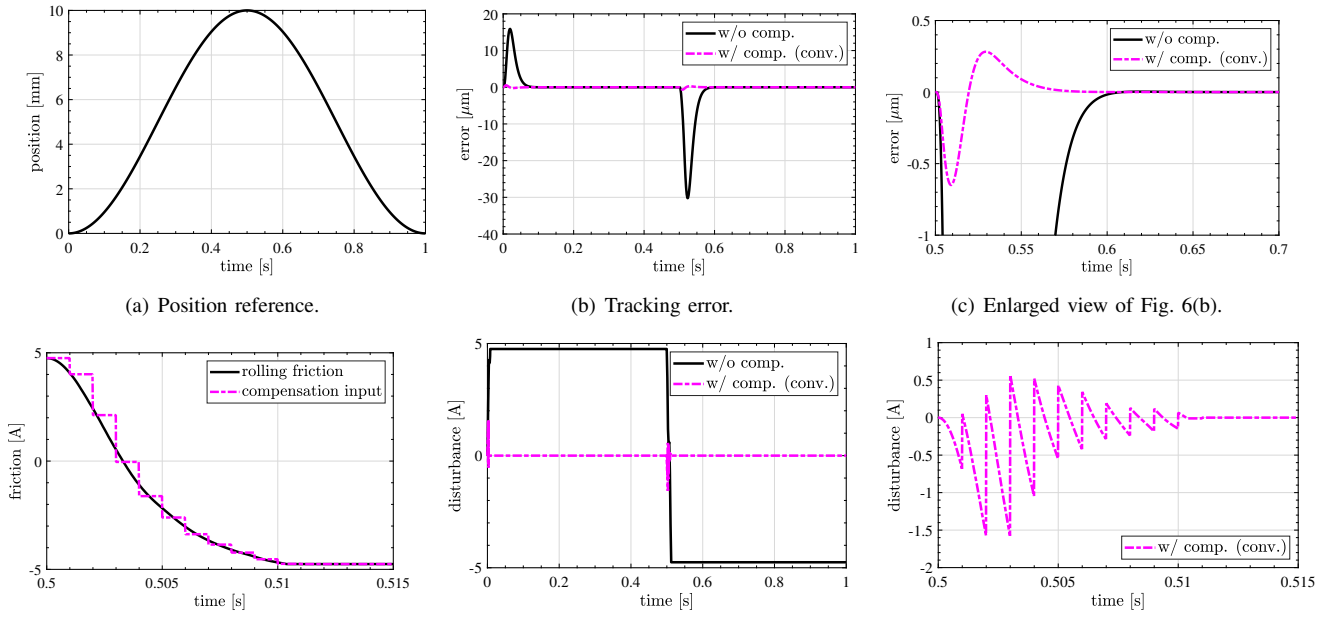

(a) Position reference.

(b) Tracking error.

(c) Enlarged view of Fig. 6(b).

(d) Applied rolling friction and its compensation input.

(e) Equivalent input disturbance.

(f) Enlarged view of Fig. 6(e).

Fig. 6. Simulation results of the inverse response analysis. It is confirmed that the model-based feedforward friction compensation causes the inverse response after the quadrant glitch ((c) ----), while the inverse response does not occur when the model-based feedforward friction compensation is not applied ((c) ——). Note that the unit of the rolling friction is converted from [N m] to [A] by using the torque constant K_{T}.

Besides, the rolling friction T_{rf} is compensated for by using the rolling friction model $\hat{T}_{\mathrm{rf}}$. The friction compensation input is calculated based on the friction model and position reference, while the rolling friction depends on the actual position and velocity.

2) Condition: The simulations are carried out with MATLAB/Simulink. The sampling period of the control input T_{s} is set to $1\,\mathrm{ms}$, and the calculation period of the simulations is set to $T_{\mathrm{s}}/100$.

The feedforward controller C_{FF} is a multirate feedforward controller [12], which is a stable inverse system of the nominal model P_{n} with a zeroth-order hold (ZOH). This feedforward controller achieves perfect tracking control if there are no modeling error nor disturbance. The feedback controller C_{FB} is designed for the closed-loop model to have the quadruple poles at $-\omega_{\mathrm{c}} = -2\pi\times 25\,\mathrm{rad/s}$ by the pole placement method, and discretized by Tustin transformation.

To compensate for the rolling friction by feedforward control, a data-based friction model $\hat{T}_{\mathrm{rf}}$ [6], as shown in Fig. 3(c), is used. In this model, the relation between the displacement from the velocity reversal point and the rolling friction is represented as a table (Fig. 5). In the model used in this study, the rolling friction is modeled by $0.1\,\mu\mathrm{m}$ when the displacement is from $0\,\mu\mathrm{m}$ to $10\,\mu\mathrm{m}$. When the compensation input of the rolling friction is designed, the table is loaded by using the position reference.

The position reference r is a sinusoidal wave with the amplitude of $5\,\mathrm{mm}$ and the frequency of $1\,\mathrm{Hz}$, $r = 5(1-\cos(2\pi t))\,[\mathrm{mm}]$, as shown in Fig. 6(a).

In the simulations of this section, no modeling errors exist, i.e., the simulation plant of the stage is the same as its model P_{n}, and the applied rolling friction is the same as its model.

3) Result: The simulations compare the case without the friction compensation (black solid lines in Fig. 6) and the case with it (magenta dash-dotted lines in Fig. 6). Fig. 6 shows the results of the simulations.

As shown in Fig. 6(b), the tracking error is suppressed due to the friction compensation; however, the inverse response occurs after the quadrant glitch, see Fig. 6(c). Fig. 6(d) shows the applied rolling friction and its compensation input around the velocity reversal timing. Fig. 6(e) and Fig. 6(f) show the equivalent input disturbance, which is defined as the difference between the applied rolling friction and its compensation input. The equivalent input disturbance is small on the sampling points; however, it is relatively large between the sampling points because the control input is discretized by ZOH.

B. Analysis

To analyze the inverse response, this subsection focuses on the equivalent input disturbance shown in Fig. 6(e) and Fig. 6(f). According to these figures, the characteristics of the equivalent input disturbance are changed by the friction compensation. The rolling friction behaves as an input step disturbance; therefore, the equivalent input disturbance is also an input step disturbance when the rolling friction is not compensated for. On the other hand, the friction compensation causes a spike-like input disturbance due to ZOH. This disturbance causes the inverse response as shown in Fig. 6(c).

Generally, the following relation holds [13]:

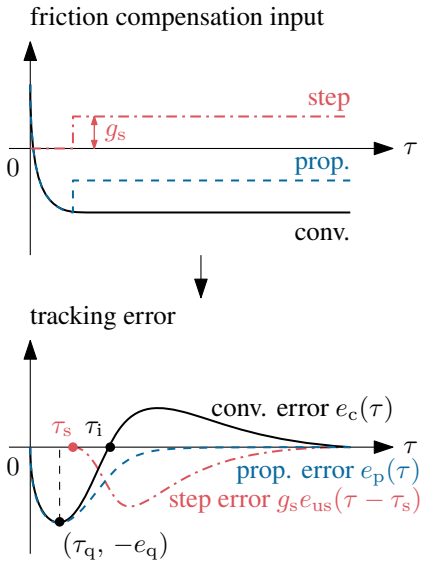

Fig. 7. Concept of the proposed approach. A step input with the size of g_s is injected at $\tau = \tau_s$ and cancels the inverse response caused by the conventional friction compensation.

Relation between Feedback Controller Structure and Input Disturbance Response: *Now we consider a closed-loop system with a linear time-invariant plant and a linear time-invariant feedback controller. Besides, we assume that the feedback controller has i integrators. Then, when an impulse input disturbance is applied, the error $e_i = r - x$ satisfies*

$$\int_0^\infty e_i(\tau)\mathrm{d}\tau = 0 \quad (i \geq 1). \tag{2}$$

Furthermore, when a step input disturbance is applied, the error $e_s = r - x$ satisfies

$$\begin{cases} \lim\limits_{\tau\to\infty} e_s(\tau) = 0 & (i \geq 1) \\ \int_0^\infty e_s(\tau)\mathrm{d}\tau = 0 & (i \geq 2) \end{cases}. \tag{3}$$

The feedback controller of the considered control system has an integrator to avoid steady-state error; therefore, the spike-like input disturbance caused by the friction compensation results in the inverse response (2) even if there are no modeling errors. By contrast, the inverse response does not necessarily occur when the friction compensation is not conducted, see (3).

In summary, the inverse response is caused by the integrator of the feedback controller and the friction compensation input discretized by ZOH.

IV. Suppression of Inverse Response

In this section, a suppression approach of the inverse response is presented. The concept of the proposed approach is shown in Fig. 7. Besides, the procedure of the proposed approach is shown in Fig. 8. The aim of the proposed approach is the suppression of the inverse response without increasing the quadrant glitch. The key idea is to add a step input to the friction compensation input and cancel the inverse response.

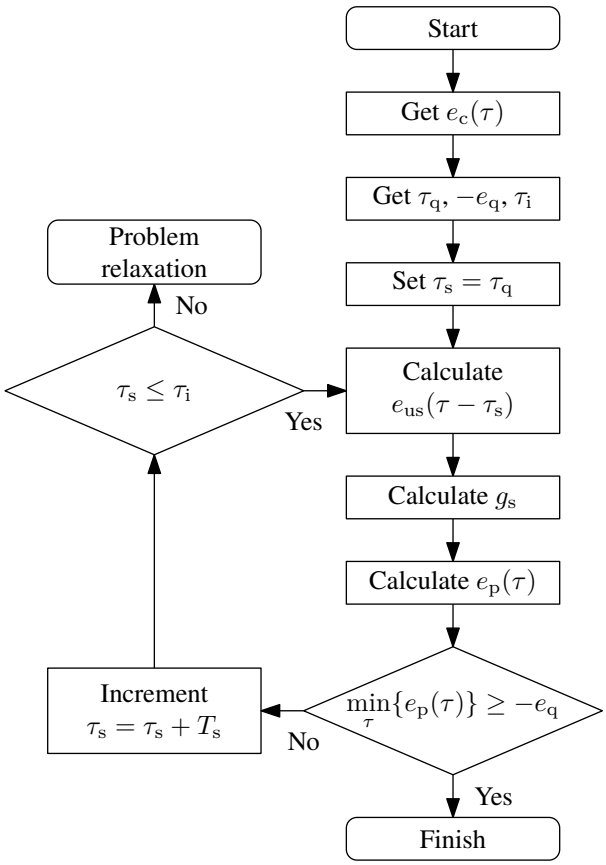

Fig. 8. Procedure of the proposed approach. After the simulation or experiment with the conventional friction compensation, the step input used in the proposed approach is tuned.

Notation. τ denotes the time and $\tau = 0$ is the velocity reversal timing of the stage. Let $e_c(\tau)$ be the tracking error caused by the conventional friction compensation, $e_{us}(\tau)$ the tracking error caused by the unit step input, and $e_p(\tau)$ the predicted tracking error caused by the proposed friction compensation. Let τ_q and e_q denote the timing and size of the quadrant glitch caused by the conventional friction compensation, τ_i the zero-cross timing of the $e_c(\tau)$, τ_s the timing when the step input is added, and g_s the size of the injected step input. The above data are depicted in Fig. 7.

A. Problem Formulation and Objective

In the proposed approach, the principle of superposition is assumed to hold. In other words, the following equation holds:

$$e_p(\tau) = e_c(\tau) + g_s e_{us}(\tau - \tau_s). \tag{4}$$

The objective is to find the two parameters, τ_s and g_s, so that the following relation satisfies:

$$-e_q \leq e_p(\tau) \leq 0, \forall\tau. \tag{5}$$

B. Calculation of Tracking Error Caused by Step Input

In the considered control system as shown in Fig. 4, the feedback controller C_{FB} is the following PID controller:

$$\begin{aligned} C_{\mathrm{FB}}(s) &= k_{\mathrm{p}} + k_{\mathrm{i}}\frac{1}{s} + k_{\mathrm{d}}\frac{s}{1+T_{\mathrm{f}}s} \\ &=: \frac{b_2 s^2 + b_1 s + b_0}{s^2 + a_1 s}, \end{aligned} \tag{6}$$

with k_{p} the proportional gain, k_{i} the integral gain, k_{d} the derivative gain, and T_{f} the time constant of the pseudo derivative. In this study, the PID controller is designed so that the closed-loop model have the quadruple poles at $-\omega_c$; therefore, the tracking error $e_{\mathrm{us}}(\tau - \tau_{\mathrm{s}})$, which is caused by the unit step input injected at $\tau = \tau_{\mathrm{s}}$, is expressed as follows:

$$e_{\mathrm{us}}(\tau - \tau_{\mathrm{s}}) = -\mathcal{L}^{-1}\left\{ S_{\mathrm{n}} P_{\mathrm{n}} \frac{1}{s} \mathrm{e}^{-s\tau_{\mathrm{s}}} \right\}, \tag{7}$$

$$\begin{aligned} S_{\mathrm{n}} P_{\mathrm{n}} &= \frac{P_{\mathrm{n}}}{1 + C_{\mathrm{FB}} P_{\mathrm{n}}} \\ &= \frac{RK_{\mathrm{T}}}{J_{\mathrm{n}}} \frac{s^2 + a_1 s}{(s+\omega_{\mathrm{c}})^4}, \end{aligned} \tag{8}$$

with S_{n} the model of sensitivity function.

From (7) and (8), $e_{\mathrm{us}}(\tau - \tau_{\mathrm{s}})$ is calculated as follows:

$$e_{\mathrm{us}}(\tau - \tau_{\mathrm{s}}) = \begin{cases} 0 \quad (\tau < \tau_{\mathrm{s}}) \\ -\dfrac{RK_{\mathrm{T}}}{J_{\mathrm{n}}} \mathrm{e}^{-\omega_{\mathrm{c}}(\tau - \tau_{\mathrm{s}})} \\ \quad \times \left\{ \dfrac{1}{2}(\tau - \tau_{\mathrm{s}})^2 + \dfrac{a_1 - \omega_{\mathrm{c}}}{6}(\tau - \tau_{\mathrm{s}})^3 \right\} \\ \quad (\tau \geq \tau_{\mathrm{s}}) \end{cases}. \tag{9}$$

C. Tuning of Timing and Size of Step Input

To satisfy the relation (5), the parameters, g_{s} and τ_{s}, are determined as shown in Fig. 8.

First, the timing of the step input τ_{s} is fixed and then, the size of the step input τ_{s}, which suppresses the inverse response, is calculated as follows:

$$g_{\mathrm{s}} = \max_{\tau \geq \tau_{\mathrm{i}}} \left\{ \frac{e_{\mathrm{c}}(\tau)}{-e_{\mathrm{us}}(\tau - \tau_{\mathrm{s}})} \right\}. \tag{10}$$

Next, it is confirmed whether the proposed approach causes larger quadrant glitch than the conventional friction compensation as follows:

$$\min_{\tau}\{e_{\mathrm{p}}(\tau)\} \geq -e_{\mathrm{q}}. \tag{11}$$

In this step, the tracking error e_{p}, which is caused by the proposed approach, is predicted as (4). If the proposed approach is expected to increase the quadrant glitch, the timing τ_{s} is incremented by the sampling period and the size g_{s} is recalculated as (10).

In the above procedure, the following condition is imposed on the timing τ_{s} to satisfy the objective (5):

$$\tau_{\mathrm{q}} \leq \tau_{\mathrm{s}} \leq \tau_{\mathrm{i}}. \tag{12}$$

If no solutions are found by the proposed approach, the objective (5) is relaxed, i.e., a small inverse response or a larger quadrant glitch is allowed.

V. Evaluation of Proposed Approach

The proposed approach is evaluated through the simulations and experiments. The simulations and experiments compares the case without the friction compensation (black solid lines in Fig. 9 and Fig. 10), the case with the conventional friction compensation described in Section III (magenta dash-dotted lines in Fig. 9 and Fig. 10), and the case with the proposed friction compensation described in this section (blue dotted lines in Fig. 9 and Fig. 10). The position reference used in the simulations and experiments is shown in Fig. 6(a).

A. Simulation

The simulations are carried out under the same conditions described in Section III. Fig. 9 shows the simulation results.

First, the tracking error e_{c}, which is caused by the conventional friction compensation, is measured. From e_{c} and the procedure shown as Fig. 8, the step input with the size of $0.1379\,\mathrm{A}$ is injected at $0.509\,\mathrm{s}$ in the proposed approach (Fig. 9(c)).

Fig. 9(a) and Fig. 9(b) show the tracking error of each case. As shown in these figures, the proposed approach suppresses the inverse response without increasing the quadrant glitch.

B. Experiment

The experiments with the setup shown in Fig. 3(a) are also carried out. The results are shown in Fig. 10.

From the tracking error caused by the conventional friction compensation, the step input with the size of $1.73\,\mathrm{A}$ is injected at $0.505\,\mathrm{s}$ (Fig. 10(c)). Owing to the step input, the proposed approach decreases the inverse response (Fig. 10(a) and Fig. 10(b)). Note that the tracking error e_{c} later than $0.54\,\mathrm{s}$ is ignored in the step input design procedure of the proposed approach to find the solution $(\tau_{\mathrm{s}},\, g_{\mathrm{s}})$. This leads to the small inverse response in the proposed approach.

VI. Conclusion

This study focuses on the inverse response caused by the conventional friction compensation. First, the inverse response caused by the model-based feedforward friction compensation is analyzed. From the analysis, it is concluded that the inverse response is caused by the integrator and control input discretized by ZOH. These causes are inevitable in the motion control application. Then, the suppression approach of the inverse response is proposed. In the proposed approach, the step input is injected to cancel the inverse response. The proposed approach is evaluated through the simulations and experiments.

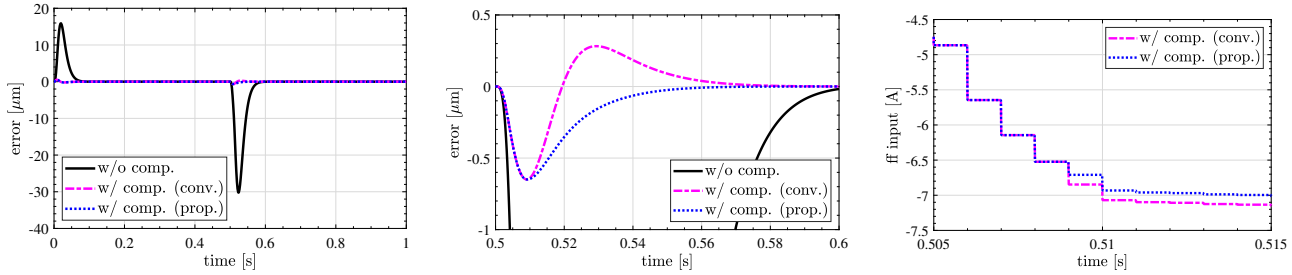

(a) Tracking error. (b) Enlarged view of Fig. 9(a). (c) Feedforward input around the velocity reversal timing of the stage.

Fig. 9. Simulation results of the inverse response suppression. The position reference is shown in Fig. 6(a). The conventional friction compensation causes the inverse response ((b) ----). In contrast, the proposed approach cancels the inverse response without increasing the quadrant glitch ((b) ·····).

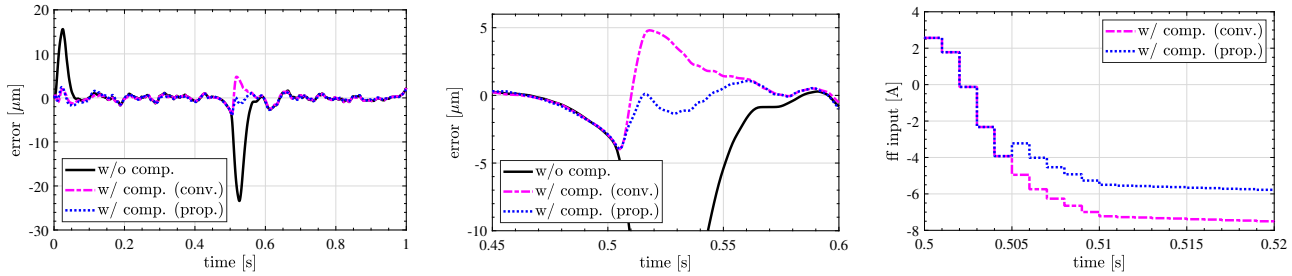

(a) Tracking error. (b) Enlarged view of Fig. 10(a). (c) Feedforward input around the velocity reversal timing of the stage.

Fig. 10. Experimental results of the inverse response suppression. The position reference is shown in Fig. 6(a). The proposed approach efficiently decreases the inverse response without increasing the quadrant glitch ((b) ·····) compared with the conventional friction compensation ((b) ----). Note that the feedforward controller C_{FF} is tuned to decrease the tracking error.

REFERENCES

[1] Y. Altintas, A. Verl, C. Brecher, L. Uriarte, and G. Pritschow, "Machine tool feed drives," *CIRP Ann.*, vol. 60, no. 2, pp. 779–796, 2011.

[2] V. Lampaert, J. Swevers, and F. Al-Bender, "Comparison of model and non-model based friction compensation techniques in the neighbourhood of pre-sliding friction," in *Proc. 2004 Am. Control Conf.* IEEE, 2004, pp. 1121–1126 vol.2.

[3] C. Canudas de Wit, H. Olsson, K. Astrom, and P. Lischinsky, "A new model for control of systems with friction," *IEEE Trans. Automat. Contr.*, vol. 40, no. 3, pp. 419–425, 1995.

[4] F. Al-Bender, V. Lampaert, and J. Swevers, "The Generalized Maxwell-Slip Model: A Novel Model for Friction Simulation and Compensation," *IEEE Trans. Automat. Contr.*, vol. 50, no. 11, pp. 1883–1887, 2005.

[5] Y. Maeda and M. Iwasaki, "Feedforward Friction Compensation Using the Rolling Friction Model for Micrometer-stroke Point-to-point Positioning Motion," *IEEJ J. Ind. Appl.*, vol. 7, no. 2, pp. 141–149, 2018.

[6] T. Takemura and H. Fujimoto, "Proposal of novel rolling friction compensation with data-based friction model for ball screw driven stage," in *IECON 2010 - 36th Annu. Conf. IEEE Ind. Electron. Soc.*, vol. 1. IEEE, 2010, pp. 1932–1937.

[7] M. Ruderman and T. Bertram, "Two-state dynamic friction model with elasto-plasticity," *Mech. Syst. Signal Process.*, vol. 39, no. 1-2, pp. 316–332, aug 2013.

[8] T. Hayashi, H. Fujimoto, Y. Isaoka, and Y. Terada, "Projection-based Iterative Learning Control for Ball-screw-driven Stage with Consideration of Rolling Friction Compensation," *IEEJ J. Ind. Appl.*, vol. 9, no. 2, pp. 132–139, 2020.

[9] H. Fujimoto and T. Takemura, "High-Precision Control of Ball-Screw-Driven Stage Based on Repetitive Control Using n-Times Learning Filter," *IEEE Trans. Ind. Electron.*, vol. 61, no. 7, pp. 3694–3703, 2014.

[10] T. Ohashi, H. Shibata, S. Futami, and R. Sato, "Quadrant glitch compensation by a modified disturbance observer for linear motor stages," *Precis. Eng.*, vol. 59, pp. 18–25, 2019.

[11] Y. Yoshiura, Y. Asai, and Y. Kaku, "Anti-resonance vibration suppression control in full-closed control system," *IEEJ J. Ind. Appl.*, vol. 9, no. 3, pp. 311–317, 2020.

[12] H. Fujimoto, Y. Hori, and A. Kawamura, "Perfect tracking control based on multirate feedforward control with generalized sampling periods," *IEEE Trans. Ind. Electron.*, vol. 48, no. 3, pp. 636–644, 2001.

[13] G. C. Goodwin, S. F. Graebe, and M. E. Salgado, "Control System Design." Prentice Hall PTR, 2000.